Metabolites from the entophytic fungus *Sporormiella minimoides* isolated from *Hintonia latiflora*

By: Martha Leyte-Lugo, Mario Figueroa, María del Carmen González, Anthony E. Glenn, Martín González-Andrade, and Rachel Mata

Leyte-Lugo, M., Figueroa, M., González, M.D.C., Glenn, A.E., González-Andrade, M., Mata, R. (2013). Metabolites from the entophytic fungus Sporormiella minimoides isolated from Hintonia latiflora. *Phytochemistry, 96,* pp. 273-278. DOI: 10.1016/j.phytochem.2013.09.006

Made available courtesy of Elsevier: https://doi.org/10.1016/j.phytochem.2013.09.006

*****© 2013 Elsevier Ltd. Reprinted with permission. This version of the document is not the version of record. Figures and/or pictures may be missing from this format of the document. *****

Abstract:

An extract of the solid cultures of *Sporormiella minimoides* (Sporormiaceae) isolated as an endophytic fungus from *Hintonia latiflora* (Rubiaceae), yielded three polyketides, 3,6-dimethoxy-8-methyl-1*H*,6*H*-benzo[*de*]isochromene-1,9-dione, 3-hydroxy-1,6,10-trimethoxy-8-methyl-1*H*,3*H*-benzo[*de*]isochromen-9-one, and 5-hydroxy-2,7-dimethoxy-8-methylnaphthoquinone, along with three known compounds, corymbiferone, ziganein, and brocaenol B. Their structures were characterized by spectrometric and spectroscopic methods. So as to be consistent the literature reports, 3,6-dimethoxy-8-methyl-1*H*,6*H*-benzo[*de*]isochromene-1,9-dione and 3-hydroxy-1,6,10-trimethoxy-8-methyl-1*H*,3*H*-benzo[*de*]isochromen-9-one were given the trivial names of corymbiferone C and corymbiferan lactone E, respectively. All isolates were tested as potential human calmodulin (*h*CaM) inhibitors using the fluorescent biosensor *h*CaM V91C-*mBBr*, but only 5-hydroxy-2,7-dimethoxy-8-methylnaphthoquinone quenched significantly the extrinsic fluorescence of this biosensor, with a dissociation constant (K_d) value of 1.55 μM. Refined docking analysis predicted that 5-hydroxy-2,7-dimethoxy-8-methylnaphthoquinone could also be bound to *h*CaM at site I displaying hydrophobic interactions with Phe19 and 68, Met51, 71, and 72, and Ile52 and 63 residues.

Graphical abstract: *Sporormiella minimoides* isolated as an endophyte from *Hintonia latiflora* yielded three polyketides, 3,6-dimethoxy-8-methyl-1*H*,6*H*-benzo[*de*]isochromene-1,9-

dione, 3-hydroxy-1,6,10-trimethoxy-8-methyl-1*H*,3*H*-benzo[*de*]isochromen-9-one, and 5-hydroxy-2,7-dimethoxy-8-methylnaphthoquinone; the latter is a *h*CaM inhibitor. Corymbiferone, ziganein, and brocaenol B were also isolated.

Keywords: Endophytic fungus | Calmodulin inhibitors | Polyketides | *Sporormiella minimoides* | *Hintonia latiflora*

Article:

1. Introduction

Sporormiella is a genus with ~80 species distributed across the boreal and temperate regions of the world. Some species of the genus are saprobes, whereas others are endophytic in living plants and fungi (Ahmed and Cain, 1972, Liang-Dong et al., 2008, Mudur et al., 2006). *Sporormiella minimoides* S.I. Ahmed & Cain (Sporormiaceae) [= *Preussia minimoides* (S.I. Ahmed & Cain) Valldos. & Guarro] (Valldosera and Guarro, 1990) has been isolated from dung, *Pinus tabulaeformis*, and *Trametes hirsutum*, a fungus collected from a dead hardwood branch in a dry forest in Hawaii (Liang-Dong et al., 2008, Mudur et al., 2006). Previous chemical investigation of this species led to isolation of several bioactive natural products including brocaenol A with cytotoxic activity (Bugni et al., 2003), a depsipeptide (Clapp-Shapiro et al., 1998) and two polyketides, sporminarins A and B (Mudur et al., 2006), with antibacterial and antifungal properties.

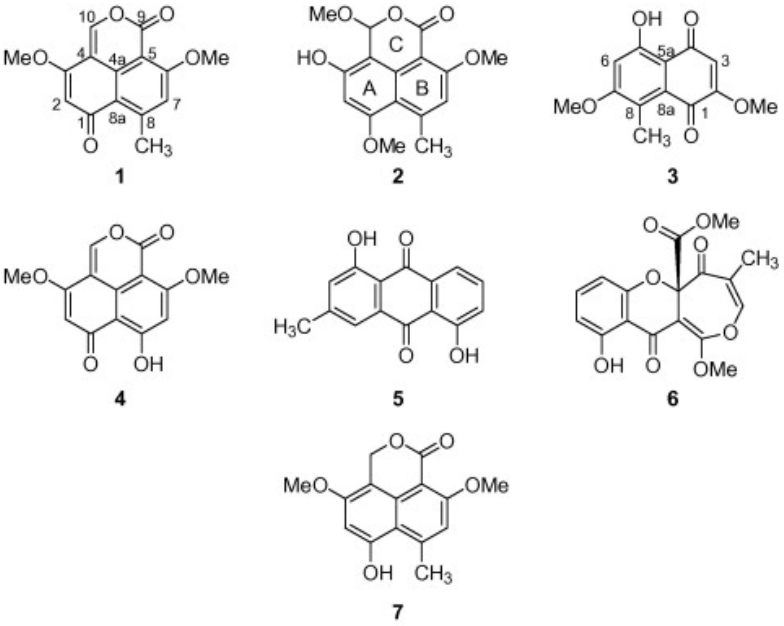

As part of our continuing search for new human calmodulin (*h*CaM) inhibitors (Figueroa et al., 2009) from the endophyte fungi from the medicinal plant *Hintonia latiflora* (Sessé et Mociño ex DC.) Bullock (Rubiaceae), another endophyte, namely *S. minimoides*, was isolated and investigated (Leyte-Lugo et al., 2012). Herein reported are the structural elucidation and potential affinity to *h*CaM of three new polyketides, 3,6-dimethoxy-8-methyl-1*H*,6*H*-

benzo[*de*]isochromene-1,9-dione (**1**), 3-hydroxy-1,6,10-trimethoxy-8-methyl-1*H*,3*H*-benzo[*de*]isochromen-9-one (**2**), and 5-hydroxy-2,7-dimethoxy-8-methylnaphthoquinone (**3**). Compounds **1** and **2** were given the trivial names of corymbiferone C and corymbiferan lactone E. The known polyketides corymbiferone (**4**) ziganein (**5**), and brocaenol B (**6**) were also identified and tested for anti-*h*CaM activity.

2. Results and discussion

S. minimoides was cultured in moist rice and extracted with CH_2Cl_2. From the crude extract corymbiferone (**4**) spontaneously crystallized; it had been previously isolated from *Penicillium hordei* (Overy et al., 2005). Extensive chromatographic separation of the mother liquors led to the isolation of compounds **1**–**3**, **5**, and **6**. Compounds **1**–**3** are novel, whereas **5** was previously reported from *Digitalis schischkinii* (Imre et al., 1974), *Salvia przewalskii* (Lu et al., 1992), *Cassia italica* (Kazmi et al., 1994), and *Aloe hijazensis* (Abd-Alla et al., 2009), and **6** from *P. brocae*; the latter compound exhibited the same optical rotation value as brocaenol B (Bugni et al., 2003).

Corymbiferone C (**1**) was obtained as a white powder. As for compound **4**, it exhibited UV absorption bands at 208, 251, 279 and 292 nm and its IR spectrum was consistent with the presence of lactone (1742 cm^{-1}) and conjugated ketone (1651 cm^{-1}) groups. The ^{1}H and ^{13}C NMR spectra of **1** (Table 1) established its structural relationship with corymbiferone (**4**) (Overy et al., 2005). The main differences between the spectra of both compounds were observed in the resonances attributable to the B ring. As expected in comparison with **4**, the signals for C-8a, C-7/H-7 and C-5 were paramagnetically shifted in **1** to δ_C 118.8, δ_C/δ_H 115.2/6.93, and δ_C 105.5, respectively. On the other hand, the resonance for C-8 was diamagnetically shifted to δ_C 152.8. The HMBC experiment (Table 1 and Fig. 1) supported placement of the methyl signal at C-8, instead of the hydroxyl group as in **4**, because long-range correlations were observed between CH_3-8 (δ_H 2.92) and C-4a (δ_C 136.6), C-7, C-8 and C-8a. In addition, H-7 was correlated with C-5, C-6 (δ_C 163.7), C-8 and C-8a. The NOESY experiment (Fig. 1) provided additional evidence to this structural proposal since cross-peaks were observed between H-7 and OCH_3-6 (δ_H 4.10) and CH_3-8. Thus compound **1** was characterized as 3,6-dimethoxy-8-methyl-1*H*,6*H*-benzo[*de*]isochromene-1,9-dione.

Table 1. ^{1}H (500 MHz) and ^{13}C (125 MHz) NMR spectroscopic data for compounds **1** and **2** in $CDCl_3$ and DMSO-d_6, respectively.

Position[a]	1				2			
	δ_C	δ_H (mult., *J* in [Hz])	HMBC[b]	NOESY	δ_C	δ_H (mult., *J* in [Hz])	HMBC[b]	NOESY
1	185.4				156.9			
2	104.1	5.86 (s)	1, 3, 8, 8a, 10	3-OMe	95.7	6.61 (s)	1, 3, 4, 8, 8a, 10	1-OMe
3	161.7				159.9			
4	108.5				102.4			
4a	136.6				133.7			
5	105.5				100.8			
6	163.7				162.5			
7	115.2	6.93 (s)	5, 6, 8, 8a, 9	6-OMe 8-Me	113.4	7.01 (s)	5, 6, 8, 8a	6-OMe 8-Me
8	152.8				147.1			
8a	118.8				112.8			
9	156.9				160.9			

Position[a]	1				2			
	δ_C	δ_H (mult., *J* in [Hz])	HMBC[b]	NOESY	δ_C	δ_H (mult., *J* in [Hz])	HMBC[b]	NOESY
10	148.2	8.06 (s)	3, 4, 4a, 9		97.5	6.18 (s)	4, 4a, 9	10-OMe
1-OMe					56.3	3.83 (s)	1	
3-OMe	55.8	3.90 (s)	2, 3, 4	2-H				
6-OMe	56.6	4.10 (s)	6, 7	7-H	56.8	3.93 (s)	6	
8-Me	24.9	2.92 (d, 1.0)	1, 4a, 7, 8, 8a	7-H	25.8	2.83 (s)	7, 8	1-OMe
10-OMe					55.5	3.31 (s)	10	
3-OH						10.78 (bs)	2, 3, 10	2-H, 10-OMe

[a] The position is related to the structure of corymbiferone (**4**).

[b] HMBC correlations are from the hydrogen stated to the indicated carbon.

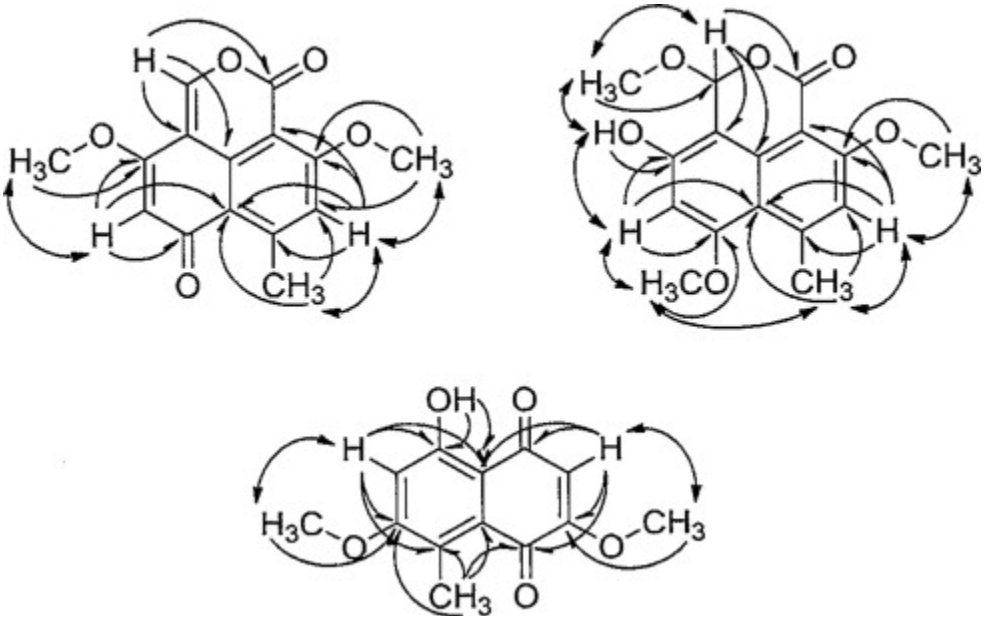

Fig. 1. Selected HMBC (→) and NOESY (↔) correlations of **1**–**3**.

Corymbiferan lactone E (**2**) was isolated as an optically inactive yellow solid. Its IR spectrum showed absorption bands for cyclic ester (1743 cm^{-1}) and conjugated ketone (1689 cm^{-1}) functionalities. The UV and NMR spectra of **2** (Table 1) showed similarities, albeit partial, to those of corymbiferan lactone D (**7**) suggesting a similar skeletal structure (Overy and Blunt, 2004). However, compound **2** had a methoxy group at C-10 (δ_C 97.5) and the disposition of the hydroxyl and methoxy groups in ring A were inverted with respect to **7**. Long-range couplings observed in the HMBC experiment (Table 1 and Fig. 1) between H-10 (δ_H 6.18) with OCH_3-10 (δ_C 55.5), and C-9 (δ_C 160.9), confirmed the placement of a methoxy group at C-10. On the other hand, NOESY correlations (Fig. 1) supported the assignment of the hydroxyl and methoxy group in ring A at C-3 and C-1, respectively, i.e. from OCH_3-10 (δ_H 3.31) to H-10 and OH-3 (δ_H 10.78); from OH-3 to H-2 (δ_H 6.61); and from OCH_3-1 (δ_H 3.83) to H-2 and CH_3-8 (δ_H 2.83). The low yield (4.4 mg) of compound **2** as an optically inactive product (i.e. as a racemic mixture) raised the possibility of it being an isolation artifact generated by the electrophilic addition of MeOH to a suitable precursor. Therefore, the structure of **2** was established as 3-hydroxy-1,6,10-trimethoxy-8-methyl-1*H*,3*H*-benzo[*de*]isochromen-9-one.

Compound **3** was obtained as orange needles. Its NMR spectra (Table 2) showed characteristic signals for a tetrasubstituted naphthoquinone derivative (Ioset et al., 1998) and in addition it had two methoxyl (δ_C/δ_H 56.5/3.88 and 56.2/3.90), one methyl (δ_C/δ_H 12.6/2.52), a hydrogen bonded hydroxyl group (δ_H 13.28), and two methines which absorb in the aromatic region (δ_C/δ_H 108.3/6.02 and 104.2/6.63). The signal at δ_H 6.63 was assigned to the quinonoid hydrogen (H-6) due its HMBC correlation with both carbonyl groups (δ_C 189.4 and 181.2) of the quinone moiety. Furthermore, correlations between H-6 and the resonance at δ_C 164.2 (C-7), and between δ_H 3.90 (7-OCH_3) with C-7 supported the placement of one of the methoxy groups at this position. The intense NOESY interaction (Fig. 1) between H-6 and 7-OCH_3 favored this proposal. Long-range interaction between H-3 (δ_H 6.02) to C-5a, C-1, C-4, and C-2 (δ_C 108.4, 181.2, 189.4, and 161.0, respectively) indicated that the aromatic hydrogen was between the chelated hydroxyl and the other methoxy group. Finally, since the methyl group hydrogens correlated with C-8a (δ_C 128.8) and C-2, the methyl group was placed at C-1. On the basis of this evidence, the compound was characterized as 5-hydroxy-2,7-dimethoxy-8-methylnaphthoquinone (**3**).

Table 2. ^{1}H (500 MHz) and ^{13}C (125 MHz) NMR spectroscopic data for compound **3** in $CDCl_3$.

Position	δ_C	δ_H (mult., *J* in [Hz])	HMBC[a]	NOESY
1	181.2			
2	161.0			
3	108.3	6.02 (s)	1, 2, 4, 5a	2-OMe
4	189.4			
5	162.8			
5a	108.4			
6	104.2	6.63 (s)	5, 5a, 7, 8	7-OMe
7	164.2			
8	126.8			
8a	128.8			
2-OMe	56.5	3.88 (s)	2	
7-OMe	56.2	3.90 (s)	7	
8-Me	12.6	2.52 (s)	1, 2, 8, 8a	
5-OH		13.28 (s)	5, 5a	

[a] HMBC correlations are from the hydrogen stated to the indicated carbon.

The affinity of metabolites **1**–**6** with *h*CaM in solution was measured using the novel fluorescent biosensor *h*CaM V91C-*mBBr.* This novel probe was developed in the same fashion as the previously reported *h*CaM M124C-*mBBr* and *h*CaM L39C-*mBBr*/V91C-*mBBr* (González-Andrade et al., 2011) biosensors (see Section 4). The results showed that only compound **3** quenched the fluorescence of *h*CaM V91C-*mBBr* in a concentration dependent-manner (Fig. 2); the calculated dissociation constant (K_d) was 1.55 μM (positive control chlorpromazine, CPZ, K_d = 0.26 μM). In order to predict the interaction of **3** with *h*CaM (pdb code 1LIN), docking studies were performed using AutoDock 4.0 software (Fig. 3) (Huey et al., 2007, Morris et al., 1998). First, the structure of **3** was optimized with the program Gaussian 09 using density functional theory method (DFT) at the B3LYP/DGDZVP level; then the ligand was docked into the entire protein. The best position (minimum binding energy) was docked in a smaller area in order to reduce the search space and model flexibility of the docking analysis. The results indicated that compound **3** binds to site I of *h*CaM, which is a different *h*CaM-binding pocket for the known inhibitors CPZ and trifluoropiperazine (TFP) (site IV; Fig. 3a) (González-Andrade et al., 2011). An analysis of the intermolecular interactions of the complex **3**-

*h*CaM, including hydrophobic and hydrogen-bonding contacts, was made using LigPlot (Fig. 3b), and suggested hydrophobic interactions with Phe19 and 68, Met51, 71, and 72, and Ile52 and 63 residues.

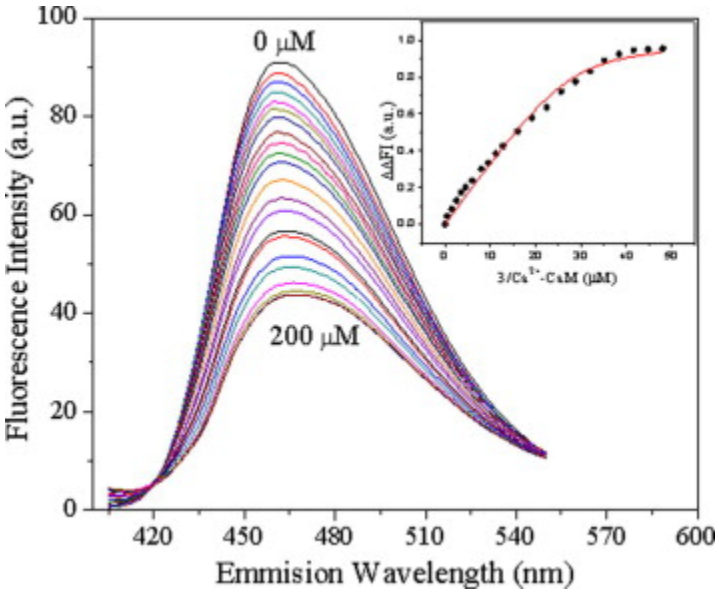

Fig. 2. Fluorescence spectra and titration curves of *h*CaM V91C-*mBBr* to saturation ion Ca^{+2} (10 mM) of **3** (0–200 μM). The absolute changes of maximal fluorescence emission were corrected for light scattering effects and plotted against the ligands to total protein ratio (insets). The continuous line in the insets comes from the fitting of data to the binding model (equation in Section 4) to obtain the K_d and the stoichiometry ratio.

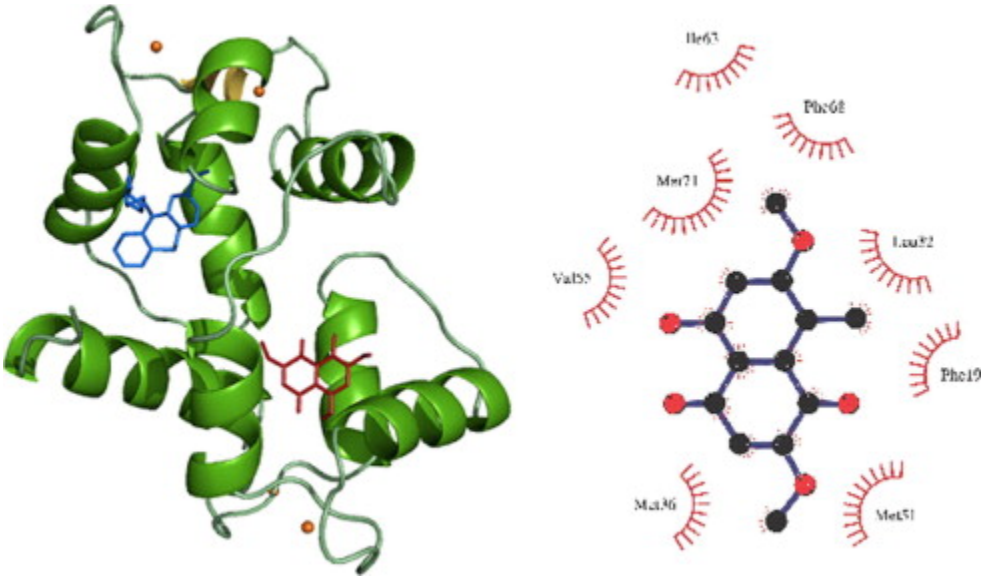

Fig. 3. Structural model of *h*CaM-TFP complex represented in green cartoon. The left panel shows the binding model of **3** (red sticks) at site I, and *h*CaM−TFP complex (blue sticks) at site IV. The right panel shows the putative interactions of amino acids of *h*CaM with **3**. (For interpretation of the references to colour in this figure legend, the reader is referred to the web version of this article.)

3. Concluding remarks

To the best of our knowledge, this is the first report of a naphthoquinone structure as a *h*CaM antagonist. The K_d, although higher than that of the positive control CPZ, is in the range of most natural products reported as *h*CaM inhibitors (Martínez-Luis et al., 2007). The chemical profile of *S. minimoides* established that the corymbiferone type of compounds is no longer restricted to the genus *Penicillum.* The presence of a methyl group at C-8, rather than a hydroxyl or carboxyl group as in compounds **1**, **2** and **7** is unusual. This structural feature might be due to post-enzymatic modifications of the original carboxyl group, leading to a reduction of this functionality, since similar compounds possessing a hydroxymethyl group at C-8 have been described in *P. hordei* (Overy and Blunt, 2004).

4. Experimental and computational

4.1. General

Melting points were determined on a Fisher-Johns apparatus and were uncorrected. IR spectra were obtained on a Perkin Elmer 400 FT-IR spectrometer, whereas the UV spectra were recorded on a Perkin Elmer Lambda 2 UV spectrometer in MeOH solution. Experimental optical rotations at the sodium D-line wavelength of pure compounds were measured in DMSO solution on a Jasco model P-1030 polarimeter at 25 °C. NMR spectra were recorded on a Varian Unity Plus 700 spectrometer at 700 (^{1}H) and 176 MHz (^{13}C), a Varian Inova-500 spectrometer at 500 (^{1}H) and 125 MHz (^{13}C), or a JEOL ECA 500 spectrometer at 500 (^{1}H) and 125 MHz (^{13}C), using TMS as the internal standard. EIMS, HRESIMS and HRFABMS were obtained on a LECO Pegasus 4D mass spectrometer, a LTQ Orbitrap XL system, injecting via a liquid chromatographic/autosampler system (Acquity UPLC), or a Thermo DFS mass spectrometer, respectively. Semi-preparative HPLC was performed using a Symmetry column (C_{18}, 7.8 × 300, 7 mm; flow rate 1.6 mL/min) and CH_3CN–H_2O (6:4), as mobile phase. Control of the equipment, data acquisition, processing, and management of chromatography was performed by the Empower 2 software (Waters). Column chromatography (CC) was carried out on either Sephadex LH-20 or silica gel (Sigma–Aldrich). Thin layer chromatography (TLC) analyses were carried out on silica gel 60 F254 plates (Merck) using ceric sulfate (10%) solution in H_2SO_4 as color reagent.

4.2. Fungal material and identification

The endophytic fungus *S. minimoides* was isolated from selected adult and healthy leaves of *H. latiflora*, collected by Sol Cristians in Huetamo (18° 31.709′N, 101° 4.692′W; 221 masl), State of Michoacan, Mexico, on July, 2010. Identification of the plant was secured by the collector; a voucher specimen (131,336) is deposited at the Herbario de la Facultad de Ciencias (FCME). A strong surface sterilization protocol was applied to the leaves (Zhang et al., 2012). Complete intact leaves were first washed with tap water to remove dust and debris and then cut into 5 × 5 mm pieces. Surface sterilization of the samples was achieved by immersing in EtOH (95:5, v/v) for 10 s, 15% NaClO for 1 min, EtOH–H_2O (75:25, v/v) for 1 min, and dried aseptically. The inner tissues were placed on isolation media (PDA, potato-dextrose agar; Difco), in Petri

dishes supplemented with penicillin (100 µg/mL) and streptomycin (100 µg/mL) to suppress bacterial growth and incubated at 25 °C until the outgrowth of endophytes was discerned. The pure fungal strain was obtained after serial transfers on PDA and deposited into the Herbario Nacional de México (MEXU), voucher number 26355.

The fungus was identified based on morphological characteristics, such as ascospore morphology. Fungal colonies were grown on Potato dextrose, oatmeal, and cornmeal agar, respectively. In all cases, colonies were analyzed after 17 days at 25 °C and 67% of relative humidity in a 12 h photoperiod. After 17 days, the fungus formed ascomata in culture. Ascospores of the fungus were cylindrical, olivaceus when young to dark brown and opaque when mature, four-celled, cells easily separable, transversely septate, with a hyaline gelatinous sheath. These forgoing morphological characters agree in all respects with the original protologue of *S. minimoides*, Pleosporales, Ascomycota, Dothideomycetes (Ahmed and Cain, 1972). Sequence data [internal transcribed spacer (ITS) and 28S ribosomal RNA] region were deposited in GenBank as accessions KF557658 and KF557659, respectively. Data available at GenBank aligning with MEXU 26355 suggested this fungus is *S. minimoides*.

4.3. Fermentation and isolation of compounds

Solid-state fermentation of the endophytic fungus *S. minimoides* was carried out in Fernbach flask containing 200 g of moist rice (white rice) cultured at 25 °C for 25 days with a 12 h daily photoperiod. The cultivated rice was extracted exhaustively with CH_2Cl_2, and the organic layer was evaporated *in vacuo*, yielding a brown solid extract (735 mg), and fraction A (891 mg) that spontaneously crystallized. The latter fraction was purified by silica gel CC with a gradient of CH_2Cl_2–MeOH (100:0–90:10) to give corymbiferone (**4**; 311 mg). The crude brown solid extract was next subjected to silica gel CC using a gradient elution of *n*-hexane–CH_2Cl_2 (100:0–0:100) and CH_2Cl_2–MeOH (100:0–90:10) to afford eight fractions (FI–FVIII). Fraction I (10.4 mg) was washed with *n*-hexane (50 mL) to obtain ziganein (**5**; 4.1 mg). Fractions III (59.9 mg), V (35.8 mg), and VII (31.4 mg) were individually subjected to Sephadex LH–20 CC eluted with MeOH to yield 5-hydroxy-2,7-dimethoxy-8-methylnaphthoquinone (**3**; 18.7 mg), brocaenol B (**6**; 5.2 mg), and corymbiferan lactone E (**2**; 4.4 mg), respectively. Fraction VI (21.5 mg) was further purified by reversed-phase HPLC to obtain corymbiferone C (**1**; 8.6 mg).

4.4. Corymbiferone C (1)

White powder; m.p. 190–192 °C; UV (MeOH) λ_{max} (log ε): 208 (4.47), 251 (4.12) 279 (4.25), 292 (4.24) nm; IR (FTIR) ν_{max}: 3474, 2924, 1742, 1651, 1614, 1582, 1465, 1353, 123, 1215 cm^{-1}; for ^{1}H and ^{13}C NMR spectroscopic data ($CDCl_3$), see Table 1; EIMS *m*/*z* (rel. int.): 272 (100, $[M]^+$), 243(47), 229 (20), 115 (15); HREIMS *m*/*z* 272.0682 (calcd for $C_{15}H_{12}O_5$, 272.0685).

4.5. Corymbiferan lactone E (2)

Yellow powder; m.p. 220–223 °C; UV (MeOH) λ_{max} (log ε): 218 (4.55), 273 (4.45) and 341 (3.91) nm; IR (FTIR) ν_{max}: 3291, 2941, 1743, 1689, 1619, 1590, 1460, 1309 cm^{-1}; for ^{1}H and ^{13}C

NMR spectroscopic data (DMSO-d_6), see Table 1; ESIMS *m/z* (rel. int.): 304 (5, $[M]^+$), 291(8), 273(100); HRESIMS *m/z* 304.0948 (calcd for $C_{16}H_{16}O_6$, 304.0947).

4.6. 5-Hydroxy-2,7-dimethoxy-8-methylnaphthoquinone (3)

Orange powder; m.p. 165–167 °C; UV (MeOH) λ_{max} (log ε) 220 (4.51), 265 (4.09) and 297 (3.96) nm; IR (FTIR) ν_{max}: 3067, 2926, 1678, 1632, 1600, 1373, 1237 cm^{-1}; for ^1H and ^{13}C NMR spectroscopic data ($CDCl_3$), see Table 2; EIMS *m/z* (rel. int.): 248 (100, $[M]^+$), 233(19), 203(19), 177 (18), 149 (15), 69 (18); HREIMS *m/z* 248.0683 (calcd for $C_{13}H_{12}O_5$, 248.0685).

4.7. Construction of *h*CaM V91C-mBBr biosensor

The construction of the *h*CaM V91C-*mBBr* biosensor was performed as described previously (González-Andrade et al., 2009, González-Andrade et al., 2011) and detailed in Supporting information.

4.8. Steady-state fluorescence using the *h*CaM V91C-mBBr biosensor

All measurements were conducted with an ISS-PC1 spectrofluorometer with sample stirring at 37 °C. The protein *h*CaM V91C-*mBBr* (5 μM) was incubated in buffer (10 mM of potassium acetate (pH 5.1) and 10 mM of $CaCl_2$) and the ligand was dissolved in DMSO (5 mM). Fluorescence emission spectra were acquired with excitation and emission slit widths of 4 and 8 nm, respectively. The excitation wavelength was 381 nm, and emission wavelengths of 420–640 nm were measured. The fractional degree of saturated *h*CaM V91C-*mBBr* with ligand (y) was calculated by changes in fluorescence on ligand binding according to $y = (F - F_0)/(F_\infty - F_0)$, where F_∞ represents the fluorescence intensity at saturation of the ligand, y is plotted as a function of the protein/ligand relation (L), and the apparent dissociation constants (K_d) and stoichiometric (S) were obtained by fitting to the equation: $y = \frac{(1+K_d/S+L/S)-\sqrt{(1+K_d/S+L/S)^2-4L/S}}{2}$ where y represents the fractional degree of fluorescence intensity at 462 nm, K_d is the apparent dissociation constant for the ligands, L is the protein/ligand relation, and S is the stoichiometric. The data were analyzed using the Origin version 8.0 program (OriginLab). Chlorpromazine (CPZ, K_d = 0.26 μM), a classical *h*CaM inhibitor, was used as a positive control.

4.9. Molecular modeling

Docking was carried using the PDB X-ray structure of *h*CaM with TFP (PDB code 1LIN.pdb). The crystal structure was rebuilt and refined after several iterations and the final all-atom refinement of *h*CaM was carried out with Rosetta 3.1.1 (Wedemeyer and Baker, 2003). The compound was built using the program Spartan'04 program (Wavefunction Inc.) and optimized geometrically using the program Gaussian 09 (Gaussian Inc.) at DTF B3LYP/DGDZVP level of theory. The protein and the ligand were further prepared using the utilities implemented by AutoDockTools 1.5.4 (http://mgltools.scripps.edu/). All hydrogen atoms and as well the Kollman united-atom partial charges were added to the structures of *h*CaM, while computing Gasteiger-Marsilli formalism charges and rotatable groups which were assigned automatically at the active torsions were added to the structures of the ligands. Blind docking was carried out using AutoDock 4.0 software (http://autodock.scripps.edu/) (Huey et al., 2007, Morris et al., 1998)

using the default parameters of Lamarkian genetic algorithm with local search, number of individuals in population (150), maximum number of energy evaluations (2.5 million), maximum number of generations (27,000), rate of gene mutation (0.02), rate of crossover (0.8), and 1000 runs for docking. Electrostatic grid maps were generated for each atom type in the ligands using the auxiliary program AutoGrid 4.0, part of the software AutoDock 4.0. The initial grid box size was 60 Å × 60 Å × 60 Å in the *x*, *y*, and *z* dimensions. Refined docking analysis was performed in a smaller grid box, with 30 Å × 30 Å × 30 Å in the *x*, *y*, and *z* dimensions, where the ligand was placed. All calculations were made using a parallel distributed memory supercomputer (KanBalam, Dirección General de Cómputo y de Tecnologías de Información y Comunicación, UNAM) [http://www.super.unam.mx/]. The analysis of the docking was made with AutoDockTools 1.5.4 using cluster analysis LigPlot (Wallace et al., 1995) and PyMOL (DeLano, 2004) programs.

Acknowledgments

This work was supported by grants from CONACyT (99395). We thank G. Duarte, M. Guzmán, M. Gutierrez, I. Rivero, A. Pérez and, Ramiro del Carmen-Lezama for their valuable technical assistance. M. Leyte-Lugo acknowledges a fellowship from CONACyT. We also thank Sol Cristians for collecting and identifying the plant material. We are indebted to Dirección General de Cómputo y de Tecnologías de Información y Comunicación, UNAM, for providing the resources to carry out computational calculations through the KanBalam System.

Appendix A. Supplementary data

Supplementary data associated with this article can be found, in the online version, at http://dx.doi.org/10.1016/j.phytochem.2013.09.006.

References

Ahmed, S.I., Cain, R.F., 1972. Revision of the genera Sporormia and Sporormiella. Can. J. Bot. 50, 419–477.

Abd-Alla, H.I., Shaaban, M., Shaaban, K.A., Abu-Gabal, N.S., Shalaby, N.M.M., Laatsch, H., 2009. New bioactive compounds from Aloe hijazensis. Nat. Prod. Res. 23, 1035–1049.

Bugni, T.S., Bernan, V.S., Greenstein, M., Janso, J.E., Maiese, W.M., Mayne, C.L., Ireland, C.M., 2003. Brocaenols A–C: novel polyketides from a marine-derived Penicillium brocae. J. Org. Chem. 68, 2014–2017.

Clapp-Shapiro, W., Burgess, B.W., Giacobbe, R.A., Harris, G.H., Mandala, S., Polishcook, J., Rattray, M., Thornton, R.A., Zink, D.L., Cabello, A., Diez, M.T., Martin, I., Pelaez, F. Antifungal agent from Sporormiella minimoides, U.S. Patent 5 801 172, September 1, 1998.

DeLano, W.L., 2004. Use of PYMOL as a communications tool for molecular science. Abstr. Pap. Am. Chem. Soc. 228, U313–U314.

Figueroa, M., González, M.C., Rodríguez-Sotres, R., Sosa-Peinado, A., González-Andrade, M., Cerda-García-Rojas, C.M., Mata, R., 2009. Calmodulin inhibitors from the fungus Emericella sp.. Bioorg. Med. Chem. 17, 2167–2174.

González-Andrade, M., Figueroa, M., Rodríguez-Sotres, R., Mata, R., Sosa-Peinado, A., 2009. An alternative assay to discover potential calmodulin inhibitors using a human fluorophore-labeled CaM protein. Anal. Biochem. 387, 64–70.

González-Andrade, M., Rivera-Chavez, J., Sosa-Peinado, A., Figueroa, M., Rodriguez-Sotres, R., Mata, R., 2011. Development of the fluorescent biosensor hcalmodulin (hCaM)L39C-monobromobimane(mBBr)/V91C-mBBr, a novel tool for discovering new calmodulin inhibitors and detecting calcium. J. Med. Chem. 54, 3875–3884.

Huey, R., Morris, G.M., Olson, A.J., Goodsell, D.S.A., 2007. Semiempirical free energy force field with charge-based desolvation. J. Comput. Chem. 28, 1145–1652.

Imre, S., Öztunç, A., Büyüktimkin, N., 1974. Ziganein und ziganein-l-methyläther: zwei neue anthrachinone aus Digitalis schischkinii. Phytochemistry 13, 681–682.

Ioset, J.R., Marston, A., Gupta, M.P., Hostettmann, K., 1998. Antifungal and larvicidal meroterpenoid naphthoquinones and a naphthoxirene from the roots of Cordia linnaei. Phytochemistry 47, 729–734.

Kazmi, M.H., Malik, A., Hammed, S., Akhtar, N., Ali, S.N., 1994. An anthraquinone derivative from Cassia italic. Phytochemistry 36, 761–763.

Leyte-Lugo, M., González-Andrade, M., González, M.C., Glenn, A.E., Cerda-García-Rojas, C.M., Mata, R., 2012. (+)-Ascosalitoxin and vermelhotin, a calmodulin inhibitor, from an endophytic fungus isolated from Hintonia latiflora. J. Nat. Prod. 75, 1571–1577.

Liang-Dong, G., Guo-Rui, H., Yu, W., 2008. Seasonal and tissue age influences on endophytic fungi of Pinus tabulaeformis (Pinaceae) in the Dongling Mountains, Beijing. J. Integr. Plant Biol. 50, 997–1003.

Lu, X.Z., Xu, W.H., Naoki, H., 1992. Anthraquinones from Salvia przewalskii. Phytochemistry 31, 708–709.

Martínez-Luis, S., Pérez-Vásquez, A., Mata, R., 2007. Natural products with calmodulin inhibitor properties. Phytochemistry 68, 1182–1903.

Morris, G.M., Goodsell, D.S., Halliday, R.S., Huey, R., Hart, W.E., Belew, R.K., Olson, A.J., 1998. Automated docking using a Lamarckian genetic algorithm and empirical binding free energy function. J. Comput. Chem. 19, 1639–1662.

Mudur, S.V., Gloer, J.B., Wicklow, D.T., 2006. Sporminarins A and B: antifungal metabolites from a fungicolous isolate of Sporormiella minimoides. J. Antibiot. 59, 500–506.

Overy, D.P., Blunt, J.W., 2004. Corymbiferan lactones from Penicillium hordei: stimulation of novel phenolic metabolites using plant tissue media. J. Nat. Prod. 67, 1850–1853.

Overy, D.P., Zidorn, C., Petersen, B.O., Duus, J.Ø., Dalsgaard, P.W., Larsen, T.O., Phipps, R.K., 2005. Medium dependent production of corymbiferone a novel product from Penicillium hordei cultured on plant tissue agar. Tetrahedron Lett. 46, 3225–3228.

Valldosera, M., Guarro, J., 1990. Estudios sobre hongos caprófilos aislados en España. XV. El género Preussia (Sporormiella). Bol. Soc. Micol. Madrid 14, 88.

Wallace, A.C., Laskowski, R.A., Thornton, J.M., 1995. LIGPLOT: a program to generate schematic diagrams of protein–ligand interactions. Protein Eng. 8, 127–134.

Wedemeyer, W.J., Baker, D., 2003. Efficient minimization of angle-dependent potentials for polypeptides in internal coordinates. Proteins 53, 262–272.

Zhang, Q., Wei, X., Wang, J., 2012. Phillyrin produced by Colletotrichum gloeosporioides, an endophytic fungus isolated from Forsythia suspensa. Fitoterapia 83, 1500–1505.